

ELECTRON BEAM DYNAMICS STUDIES FOR ELI-NP GBS LINAC

A. Giribono^{*1}, G. Campogiani¹, F. Cardelli¹, L. Palumbo¹, L. Piersanti¹, A. Vannozzi¹

Dept. SBAI “La Sapienza” University, Via Antonio Scarpa,14 00161 Rome, Italy¹ and

INFN-Roma1, Piazzale Aldo Moro,2 00161 Rome, Italy

A. Bacci, C. Curatolo, I. Drebot, V. Petrillo, A.R. Rossi, L. Serafini, Via Celoria 16, 20133 Milan, Italy

D. Alesini, A. Gallo, C. Vaccarezza, A. Variola,

INFN-LNF, Via Enrico Fermi,40 00044 Frascati Rome, Italy

Abstract

The ELI-NP Gamma Beam System (GBS) is an advanced gamma ray source based on the Compton backscattering effect with unprecedented specifications of brilliance ($>10^{21}$), monochromaticity (0.5%) and energy tunability (0.2 - 19.5 MeV), presently under construction in Magurele, Bucharest (RO). Here the head on collision is foreseen between an intense high power laser beam and a high brightness high quality electron beam with a maximum kinetic energy of 740 MeV. The electron beam dynamics analysis and control for the ELI-NP GBS Linac in the single and multi bunch mode have been investigated and are here illustrated.

INTRODUCTION

The ELI-NP Gamma Beam System (GBS) is a high spectral density and monochromatic γ photon source based on the Inverse Compton Scattering phenomenon whose main parameters are listed in Table 1. Here the challenging requirements of high spectral density leads to operates at 100 Hz repetition rate for the RF in the multi-bunch configuration. Indeed the use of a multi-bunch train colliding with a high intensity recirculated laser pulse allows to increase the number of collision per second, and so the gamma flux. In the first part of this paper the electron beam dynamics analysis and control for the ELI-NP GBS Linac will be described in the single bunch operation; in the following the case of a multi-bunch configuration will be investigated.

ELECTRON BEAM DYNAMICS

The chosen electron beam parameters needed to delivery the final source design reported in ELI-NP official Technical Design Report (TDR) [1] and listed in Table 1 are: normalised transverse emittance, ϵ_n , in the range 0.2 – 0.6 mm mrad, relative energy spread, $\Delta\gamma/\gamma$, $\leq 0.1\%$, energy tunability in the range 75 – 740 MeV, and spot size, σ_t , in the range $15 \mu\text{m} \leq \sigma_t \leq 30 \mu\text{m}$, as indicates the behavior of the source spectral density as function of the electron beam spot size analysed in chapter 1 of [1].

The preservation of the electron beam quality has been ensured adopting an hybrid scheme consisting in a SPARC-like S-band high brightness photoinjector [2] followed by a C-band RF linac as shown in Fig.1. The reason lies in having a bunch long enough, $\sigma_z \approx 1\text{mm}$, in the RF gun to reduce the emittance degradation due to the space charge

Table 1: Summary of ELI-NP GBS specifications

Energy	0.2 – 19.5	MeV
Spectral Density	$0.8-4.0 \cdot 10^4$	ph/s·eV
Bandwidth [r.m.s.]	≤ 0.5	%
Source size [r.m.s.]	10 – 30	μm
Pulse length [r.m.s.]	0.7-1.5	ps
# photons/shot within		
FWHM bandwidth	$\leq 2.6 \cdot 10^5$	
# photons/second within		
FWHM bandwidth	$\leq 8.3 \cdot 10^8$	

contribution, but taking advantage of the higher accelerating gradients provided by the C-band accelerating sections in the rest of the linac to compact its length. Hence, a bunch short enough, $\sigma_z \leq 280 \mu\text{m}$, to avoid the energy spread dilution due to RF curvature degradation effects, has been injected in the C-band linac thanks to the adoption of the velocity bunching scheme in the S-band injector resulting in a gentle compression factor ≤ 3 at the photoinjector exit. The S-band injector, operating at 2.856 GHz, is composed of a 1.6 cell S-band RF gun equipped with a copper photo cathode and an emittance compensation solenoid, followed by two TW SLAC type S-band sections. The RF gun accelerating field is $E_{acc} \approx 120 \text{ MV/m}$, while the two S-band structures can operate at a maximum of 23.5 MV/m allowing to reach a maximum electron beam energy at the injector exit of 146 MeV. The downstream C-band RF linac operates at 5.712 GHz, with the accelerating structures designed and developed at LNF, [3], where the accelerating gradient can be set up to a maximum of 33 MV/m, allowing enough margin for the off crest minimization of the energy spread in the 75 – 740 MeV energy range [4, 5]. The C- band linac is divided in two main sections as shown in Fig.1: the low energy one, composed of four accelerating sections, carries the electron beam up to the maximum energy $E = 320 \text{ MeV}$; a dogleg transport line downstream its exit, delivers the beam at the Low Energy Interaction Point (LE IP), avoiding in this way the bremsstrahlung radiation contribution. The downstream high energy linac is composed of eight accelerating sections and brings the electron beam up to the maximum energy $E = 740 \text{ MeV}$, then the electron beam, passing through a second dogleg beamline, reaches the High Energy Interaction Point (HE IP). In each of the two IP's regions a quadrupole triplet provides a flexible final focusing for matching the electron beam spot size vs the counter-propagating laser pulse.

* anna.giribono@roma1.infn.it

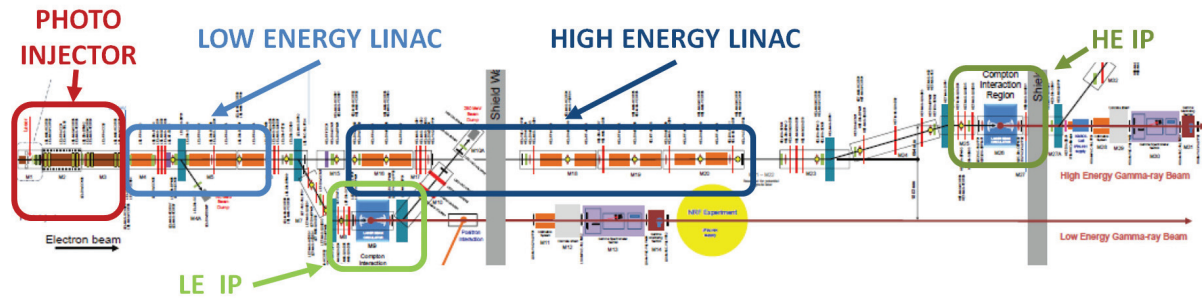


Figure 1: ELI-NP Gamma Beam System (GBS) layout: a SPARC-like S-band high brightness injector [2] followed by two C-band RF linacs (low and high energy) that through the relative transfer lines provide the electron beam to the Low and High Energy Interaction Points (LE IP and HE IP) respectively [1].

The beam dynamics for the electron beam in the injector has been simulated with Tstep [6] and Astra code [7] able to take into account the space charge effects, relevant at very low energies; C-band RF linac simulations are performed with the Elegant code [8] that includes the wakefields generated by the electron beam inside the accelerating structures together with the longitudinal space charge and the coherent and incoherent synchrotron radiation effects in the bending magnets.

Single Bunch Operation

The electron beam dynamics in the single bunch operation has been simulated for several Working Points (WPs) each corresponding to the user required γ -photon beam energy and described in details in [9, 10]. In the following we will focus on the beam dynamics of the nominal 250 pC electron beam tracked up to the LE IP with a final energy of 312 MeV, required at the LE IP for the 3.5 MeV γ photon beam production. The solenoid surrounding the first S-band cavity set at ≈ 0.4 T together with the two S-band cavities set at 23.5 MV/m in the velocity bunching scheme provide a 91.5 MeV electron beam at the injector exit with $\epsilon_n = 0.41$ mm mrad, and $\sigma_z = 280 \mu\text{m}$. In Fig.2 is plotted the evolution along the injector of the electron beam transverse normalized emittance (ϵ_n red line), spot size (σ_t blue dotted line) and longitudinal bunch length (σ_z green dashed line) as obtained with the Tstep code. The C-band accelerating cavities set at 32 MV/m with a dephasing of almost ± 10 degree with respect to the maximum RF accelerating field allow to reach energy of 312 MeV with an energy spread values of 0.080 % at LE IP. The beam transport line has been matched to correct the horizontal dispersion at the dogleg exit and the final focusing system provides an electron beam with $\sigma_t = 19.4 \mu\text{m}$ and $\epsilon_n = 0.43$ mm mrad at the LE IP. The simulation results are shown in Fig.3 and Fig.4 for the 312 MeV electron beam.

Multi-bunch Operation

The multi-bunch operation at the ELI-NP GBS foresees the head-on collision of a train of 32 electron bunches, separated by almost 16 ns, with a high intensity recirculated

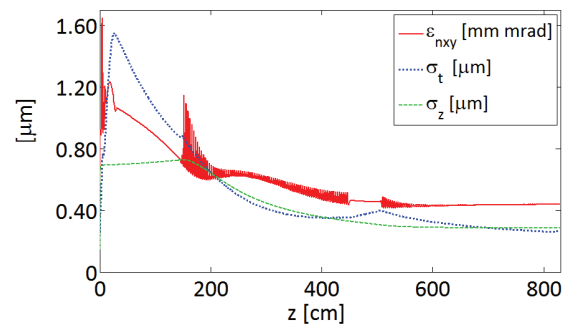


Figure 2: Simulation results for the injector: evolution along the injector of the electron beam transverse normalized emittance (ϵ_n red line), spot size (σ_t blue dotted line) and longitudinal bunch length (σ_z green dashed line) as obtained with the Tstep code.

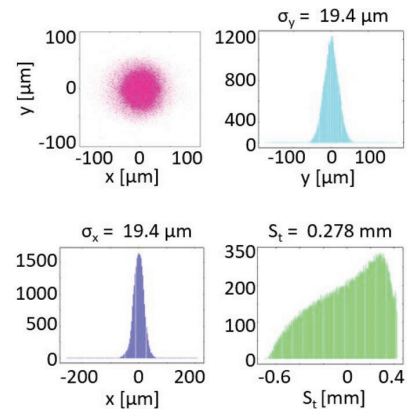


Figure 3: Simulation results for the optimised 312 MeV electron beam: simulated transverse spot size and longitudinal bunch length as obtained with Elegant tracking code.

laser pulse and allows to increase the gamma flux. In such multi-bunch configuration long-range wake fields, excited when a beam passes through the C-band linac cavities, can strongly affect the beam dynamics of the bunches trailing the first one. Longitudinal wake fields, related to the excitation of the fundamental accelerating mode and referred to

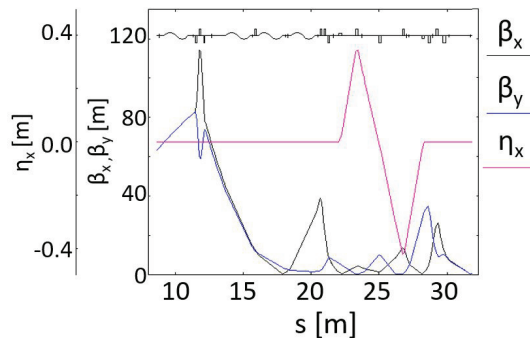


Figure 4: Simulation results for the optimised 312 MeV electron beam: simulated Twiss parameters as obtained with Elegant tracking code.

as beam loading effects, can produce a cumulative energy deviation from the first to the last bunch, while transverse wake fields can drive to the multi-bunch beam break up in case off-axis trajectories occur. The analysis has been done in terms of variation of the bunch energy along the train in the case of on-axis electron beam motion so that the effects of transverse long-range wake fields can be neglected. In detail, as reported in the Introduction of [1], the electron beam energy variation along the train is required to be lower than 0.1 % with a relative energy spread lower than 0.1 %. The electron beam dynamics of each bunch of the train has been simulated with the Elegant code superimposing the long-range wake fields to the short-range wake fields in each cell of the C-band linac accelerating structures. The longitudinal wake fields propagation inside the C-band accelerating cavities has been accurately calculated at different instances corresponding to the n^{th} bunch arrive ($n=0,1, \dots, 20$); this calculation together with a full beam loading compensation technique have been described and proposed in [11] for the ELI-NP GBS case. Since after the passage of 20 bunches the wake field reaches a steady state, the study regarded the calculation of the beam loading in case of maximum 20 bunches, not expecting observable deviation from the bunch 20^{th} to the last of the train.

In Fig.5 is plotted the simulated cumulative energy deviation in the multi-bunch operation from the first to the bunch 6^{th} due to the beam loading effect: the energy decreases from the first to the 6^{th} bunch of the train, resulting in a deviation from the first bunch energy of almost 0.2 %, reaching values higher than the 0.1% required in [1]. Also a variation in the relative energy spread along the train is expected due to the beam loading effect; in Fig.6 is plotted the relative energy spread in the multi-bunch operation from the first to the bunch 6^{th} due to the beam loading effect: the relative energy spread increases from the first to the 6^{th} bunch, reaching energy spread values higher than 0.1% required in [1].

The full beam loading compensation technique proposed in [11] can avoid this energy modulation along the train reducing the longitudinal phase space degradation at the collision with the laser pulse.

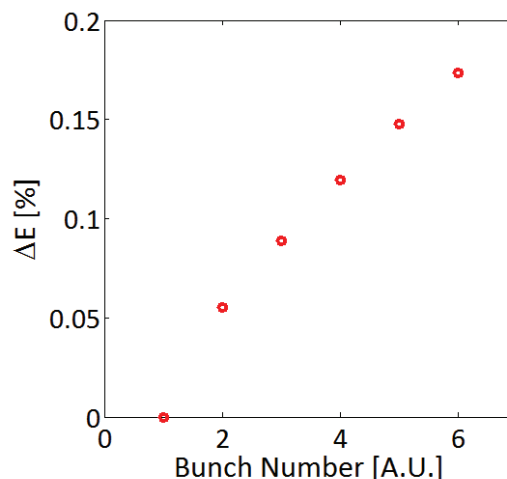


Figure 5: Cumulative energy deviation in the multi-bunch operation from the first to the last bunch due to longitudinal long-range wake fields.

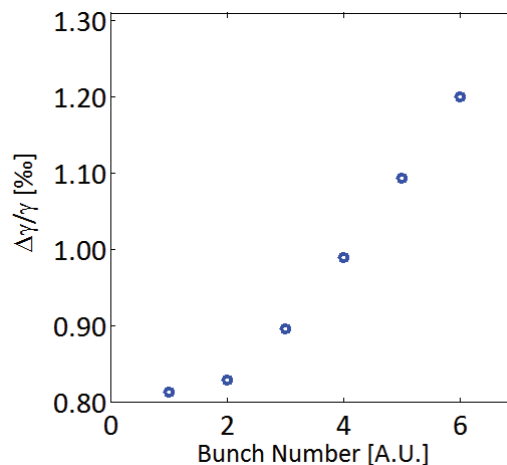


Figure 6: Relative energy spread in the multi-bunch operation from the first to the last bunch due to longitudinal long-range wake fields.

CONCLUSION

The beam dynamics has been described in both the single and multi-bunch operation. In particular, the study of the longitudinal beam dynamics in the multi-bunch operation shows an energy modulation along the bunch train and leads to take care of the beam loading effect, underlining the importance of the full beam loading compensation proposed in [11]. In the next future the study will be enlarged to the electron beam dynamics in the RF gun and in the two S-band SLAC type TW cavities. Further the transverse long-range wake fields will be treated in order to estimate the multi bunch beam break up effect on the transverse phase space.

REFERENCES

- [1] L. Serafini *et al.*, “Technical Design Report: EuroGammaS proposal for the ELI-NP Gamma beam System”, 2014.
- [2] M. Ferrario *et al.*, “Experimental Demonstration of Emittance Compensation with Velocity Bunching”, *Phys. Rev. Lett.*, vol. 104, no. 5, p. 054801, 2010.
- [3] D. Alesini *et al.*, “Design and RF Test of Damped C-Band Accelerating Structures for the ELI-NP Linac”, in *Proc. 5th Int. Particle Accelerator Conf. (IPAC'14)*, 2014, paper THPRI042
- [4] Bacci, A. *et al.*, “Electron Linac design to drive bright Compton back-scattering gamma-ray sources”, *Journal of Applied Physics*, vol. 113, no. 19, 2013.
- [5] C. Vaccarezza *et al.*, “Optimizing RF linacs as drivers for inverse Compton sources: the ELI-NP case”, in *Proc. LINAC '14*, 2014
- [6] Lloyd M. Young, *TStep*, “An electron linac design code, LMY TECHNOLOGY
- [7] K. Floetmann, [http://desy.de/~sim\\$mpyflo/Astra_dokumentation](http://desy.de/~sim$mpyflo/Astra_dokumentation)
- [8] M. Borland, *Elegant: A flexible SDDS-compliant code for accelerator simulation* Advanced Photon Source LS-287, 2000
- [9] A. Giribono *et al.*, “6D phase space electron beam analysis and machine sensitivity studies for ELI-NP GBS”, *Nucl. Instr. Meth. A*, 2016.
- [10] C. Vaccarezza *et al.*, “Optimization Studies for the Beam Dynamic in the RF Linac of the ELI-NP Gamma Beam System” presented at the 7th Int. Particle Accelerator Conf. (IPAC'16), Busan, Korea, May 2016, paper TUPOW041, this conference.
- [11] L. Piersanti *et al.*, “The RF System of the ELI-NP Gamma Beam Source” presented at the 7th Int. Particle Accelerator Conf. (IPAC'16), Busan, Korea, May 2016, paper MOPMW006, this conference.